J Appl Electrochem (2009) 39:303–309
DOI 10.1007/s10800-008-9673-5

ORIGINAL PAPER

EIS investigation of the deposition of trivalent chromium coatings on Al 6063 alloy

Hui Cheng Yu · Bai Zhen Chen · Xi Chang Shi · Hai Ying Wu · Bin Li

Received: 19 March 2008 / Accepted: 29 September 2008 / Published online: 15 October 2008

Abstract The influence of five variables (i.e. deposition temperature, time, bath pH, and concentrations of Cr^{3+} compound ($KCr(SO_4)_2$) and H_3PO_4) on the preparation of Cr^{3+} coating on Al 6063 alloy was investigated using AC impedance spectroscopy (EIS) in 3.5 wt% NaCl. The optimal conditions were determined by AC impedance spectroscopy. The results indicated that the formation and quality of the coating were very sensitive to the deposition bath pH. A mechanism was proposed to explain the results. A simple model was derived and experimentally tested in terms of an equivalent circuit. Good agreement was found between the model predictions and the experimental results. The morphologies of the coated and uncoated electrodes were examined by scanning electron microscopy (SEM), and the results also support the proposed surface model.

Keywords Chemical conversion coating · Al alloy · Trivalent chromium · EIS · Corrosion resistance

1 Introduction

Pure aluminum has a thin surface oxide layer which is generally stable in air and aqueous solution, but it lacks some necessary mechanical and physical properties, such as high specific strength, specific modulus of elasticity, creep strength, fatigue strength, hardness, wear resistance and low thermal expansion [1, 2]. Therefore pure aluminum is often alloyed with other elements for engineering applications. The protection imparted by the surface oxide to the Al substrate tends to decrease when Al is alloyed with other elements [3]. This leads to further advancements in the development of effective and economic use of surface modification technologies with the aim of improving the corrosion resistance.

Traditionally, chromate (Cr^{+6}) conversion coatings have been successfully used on Al alloys and other metals such as Zn and steel to improve the corrosion resistance [4, 5]. However, Cr^{+6} species are toxic, and European Union has prohibited them in the electrical and electronic industries [6]. Therefore the need for more environmentally friendly processes has led to the development of various Cr^{+6}-free candidates [7–11]. Recent research covers a wide variety of new chemical conversion coatings, including Ti, Mo, W, Co, Sn, Zn compounds and rare earth metal salts. All these elements are of low toxicity and are relatively abundant in nature [12–15].

EIS has widely been used for investigating the corrosion resistance of metals and inhibitors in corrosive media. Hamdy et al. studied the electroless deposition of ternary Ni–P alloy coatings containing tungsten or nano-scattered alumina composite on steel with EIS [16]. Hassani et al. investigated the effects of saccharin on the electrodeposition of Ni–Co nanocrystalline coatings [17]. Sulka et al. carried out an EIS study of barrier layer thinning in nanostructured aluminum [18]. Hasenay et al. investigated the growth kinetics and properties of potentiodynamically formed thin oxide films on aluminum in citric acid solutions by analysis of AC impedance spectra [19]. Hazzazi

H. C. Yu (✉) · B. Z. Chen · X. C. Shi
School of Metallurgical Science and Engineering, Central South University, Changsha 410083, China
e-mail: phdyhc@126.com

H. Y. Wu
Guangzhou Non-Ferrous Metal Research Institute, Guangzhou 510651, China

B. Li
Center of Modern Testing and Analysis, Central South University, Changsha 410083, China

studied the influence of the concentration of sodium succinate (SS) on the corrosion and spontaneous dissolution of copper in aerated non-stirred highly concentrated (5.0 M) NaCl solutions [20].

Recently, patents for trivalent chromium coatings on Al alloys have been reported [21, 22]. However, further study on the mechanism has rarely been reported. A new process for trivalent chromium conversion coatings on Al 6063 alloy has been developed by us, and the valence state of the coating was analyzed by X-ray photoelectron spectroscopy (XPS) [23]. The aim of this work is to derive a simple and clear model and to investigate optimum conditions for trivalent chromium (Cr^{+3}) coating using EIS in corrosive media. A mechanism is also proposed to explain the EIS results. Scanning electron microscopy (SEM) is used to analyze the morphologies of the coated and uncoated electrodes and to confirm the model.

2 Experimental procedure

2.1 Materials

Commercial Al 6063 alloy was used as a substrate for the trivalent chromium coating. The major alloying elements are given in Table 1.

2.2 Surface modification process

The trivalent chromium conversion coating process involved the following steps: polished with 600#, 800#, 1000#, 1200# abrasive paper → degreased (5 min) → rinsed with distilled water (2 min) → activated by immersion in 5% NaOH aqueous solution for 2 min → rinsed with distilled water (2 min) → immersed in the solution containing trivalent chromium compound (Cr^{+3}) → rinsed with distilled water (2 min) → dried in air (1 h) → testing (electrochemical or SEM). The deposition bath pH was adjusted with 15% NaOH and 10% H_2SO_4 to specific values. The variables investigated were: (a) temperature, (b) time of deposition, (c) bath pH and concentrations of (d) trivalent-chrome compound ($KCr(SO_4)_2$) and (e) H_3PO_4. The deposition parameters were adjusted as shown in Table 2.

2.3 EIS measurement

Prototypes were cut as cylindrical rods and mounted in glass tubes of appropriate diameter with epoxy resin. EIS experiments were performed using an electrochemical workstation from CHI Instruments (Cordova, USA), model 660B. Experiments were conducted at room temperature. The EIS of the coated and uncoated samples were measured in 3.5% NaCl aqueous solution with pH 6.2. A three-electrode cell was used. The test materials were used as the working electrodes. A large platinum foil and saturated calomel electrodes (SCE) were used as the counter and reference electrodes, respectively. AC impedance spectra were recorded in the frequency range 100 kHz–0.01 Hz, with an AC amplitude of 5 mV at the open circuit potential. AC impedance spectra were collected at constant potential conditions.

2.4 Surface analysis

Surface morphologies of the Cr^{+3} conversion coatings were observed using a JEOL JSM-6360 scanning electron microscope at an accelerating voltage of 20 kV.

3 Results and discussion

3.1 Model and testing

A complex model for hexavalent chromium (Cr^{+6}) coating on Al alloys has been proposed in the literature [24]. In

Table 1 Major alloying elements of aluminum 6063 alloy (wt%)

Si	Mg	Cu	Mn	Ni	Fe	Cr	Zn	Ti	Al
0.443	0.635	<0.030	0.040	<0.003	0.190	<0.002	<0.002	<0.002	Balance

Table 2 Parameters of conversion coating process

Item	$[KCr(SO_4)_2]$ (g L^{-1})	$[H_3PO_4]$ (g L^{-1})	pH	T (°C)	t (min)
(a) → Fig. 3a	20	20	2.0	20, 30, 40, 50	9
(b) → Fig. 3b	20	20	2.0	40	3, 6, 9, 12
(c) → Fig. 3c	20	20	1.0, 2.0, 3.0, 4.0	40	9
(d) → Fig. 3d	5, 15, 25, 35	20	2.0	40	9
(e) → Fig. 3e	20	5, 10, 20, 30	2.0	40	9

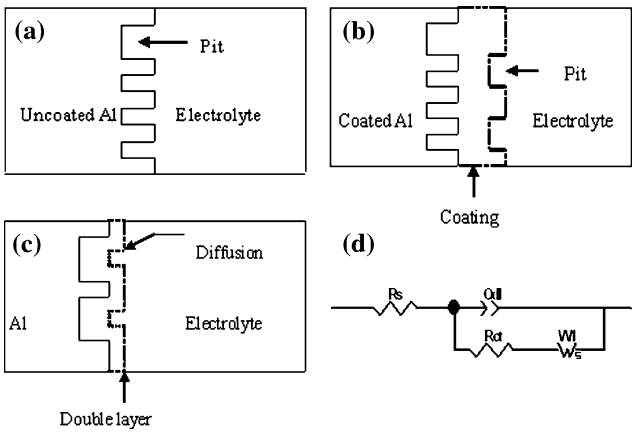

Fig. 1 Scheme of Al 6063 alloy (**a**) uncoated, (**b**) coated with trivalent chromium (Cr^{+3}), (**c**) electrode/solution interface model, and (**d**) equivalent circuit model based on the surface model

order to illustrate the mechanism of corrosion protection, a simple model based on our experiment procedure and data has been proposed by us. A graphic representation of (a) uncoated, (b) coated with trivalent chromium (Cr^{+3}), (c) electrode/solution interface model and (d) the equivalent circuit is shown in Fig. 1. *R*s represents the electrolyte resistance. The constant phase element (CPE) Q_{dl} is associated with the double layer capacitance. *R*ct models the charge transfer resistance. A classical finite-space diffusion model (*W*s) was used to describe diffusion impedance [25]. *R*w, *C*w and n_w represent diffusion impedance, capacitance and exponent of capacitance, respectively. The equivalent circuit is believed not to be affected by the modification of the electrode surface. Only the *Q*dl, *n*, *R*ct and *W*s data would be changed.

The general impedance expression describing the behavior of the distributed circuit element may be given as $Z(\omega) = A^{-1}(j\omega)^{-n}$. The boundary value of $n = 1$ corresponds to an ideal case of no dispersion and *A* becomes equivalent to a true capacitance. The value of *n* ($1 \geqq n \geqq 0$) is related to the contribution from the roughness of the electrode surface. *Q*dl is associated with non-homogeneity of the surface [19].

Generally, higher *n* and lower *Q*dl values point to a relatively high degree of surface homogeneity and yield an almost closed capacitive arc. In contrast, the lower exponent *n* and higher *Q*dl values are responsible for poor surface homogeneity, presenting a depressed arc. As an absolutely smooth electrode is impossible, the surface tends to be rough and non-homogenous as shown in Fig. 1a, b. A more homogeneous and uniform surface would result in a decreased *Q*dl and increased *n* [20].

The electrodes uncoated and coated with the second deposition condition shown in Table 2d were selected as simulated targets. The electrochemical data were tested in terms of the equivalent circuit shown in Fig. 1d. Simulated data are shown in Table 3. Nyquist plots of experimental and simulated data are shown in Fig. 2a, b. The experimental results are well matched with the equivalent circuit shown in Fig. 1d. Many pits and pores exist on the surface as described in the literature [26]. The rough surface would be covered by the more uniform coating. The fitting results support the proposed surface model and its equivalent circuit.

3.2 Effect of experimental variables

The electrodes were prepared at different (a) temperatures, (b) times, (c) bath pH and concentrations of (d) $KCr(SO_4)_2$ and (e) H_3PO_4. Figure 3 shows the AC impedance spectra obtained in 3.5% NaCl solution at room temperature. The parameters obtained by fitting the equivalent circuit are listed in Tables 3 and 4.

Table 3 Fitting results with different reacting conditions

Condition	*R*s (Ω cm^2)	*Q*dl		*R*ct (kΩ cm^2)	*W*s		
		C_{dl} (μF cm^{-2})	*n*		*R*w (kΩ cm^2)	*C*w (F cm^{-2})	n_w
Uncoated	47.6	3.40	0.87	9.9	74.1	14.1	0.53
T (°C)							
20	47.5	0.71	0.88	225.0	150.3	49.4	0.50
30	47.3	0.52	0.92	286.1	152.1	50.3	0.50
40	46.6	0.39	0.91	340.3	139.9	41.2	0.50
50	46.0	0.69	0.86	115.6	141.6	49.5	0.40
t (min)							
3	47.3	0.79	0.88	115.3	151.6	55.2	0.50
6	46.4	0.52	0.91	252.1	121.5	45.1	0.50
9	46.6	0.39	0.91	340.3	139.9	41.2	0.50
12	46.1	0.39	0.92	399.9	132.5	50.4	0.40

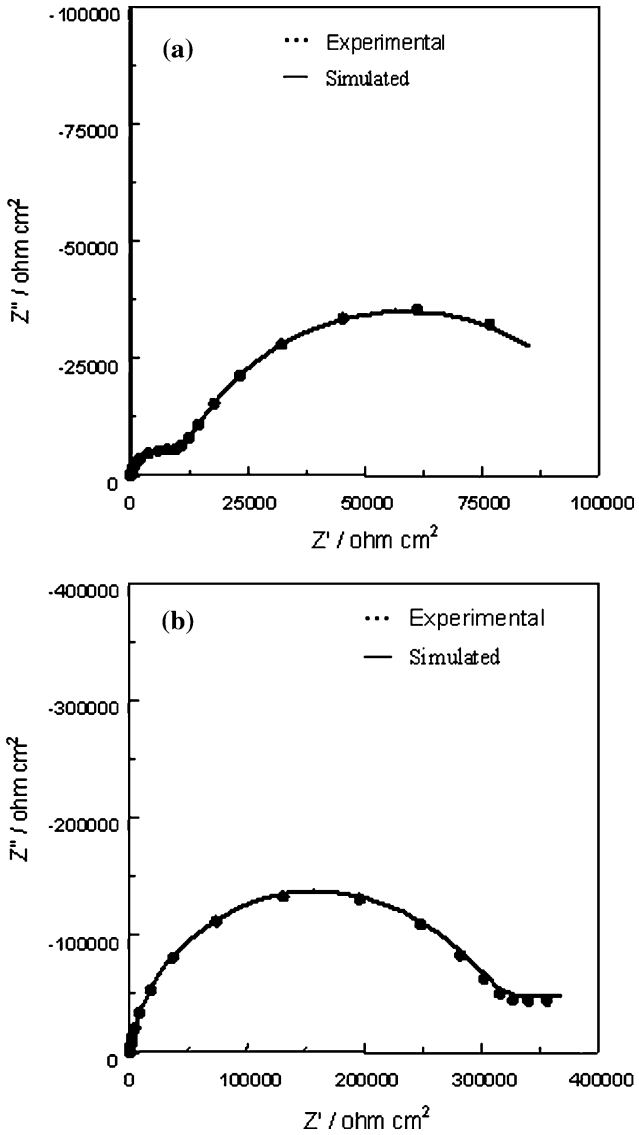

Fig. 2 Nyquist plots of the experimental and simulated data, (**a**) uncoated and (**b**) coated with pH = 2.0, 40 °C, 9 min, 15 g L^{-1} $KCr(SO_4)_2$, and 20 g L^{-1} H_3PO_4

From Fig. 3a, it can be seen that the size of the loops first increases with increasing deposition temperature from 20 to 40 °C and then decreases at 50 °C. Figure 3d, e indicate similar phenomena with increasing concentrations of $KCr(SO_4)_2$ or H_3PO_4. Tables 3 and 4 show that the variations of *R*ct and *n* values with the above deposition conditions also have similar regularity. *Qdl* initially decreases and then rises. The variation of the charge transfer (*R*ct) value can be ascribed to some extent to the change in the thickness and density of the coating. Charge transfer between the coating and solution becomes more difficult as a thicker and denser coating covers the electrode surface. Since corrosion involves diffusion and chemical reactions in the solution and electrochemical reactions at the metal surface, the thicker and denser coating can suppress O_2 and water diffusion from the external solution into the metal substrate through the pores [26].

The variations of *Q*dl, *n* and *R*ct values with different experimental conditions imply two processes for coating growth and pitting development during coating formation. It also shows that there is an optimal condition in the deposition of Cr^{+3} coating. Initially, an increase in the observed variables (temperature or concentrations of $KCr(SO_4)_2$ or H_3PO_4) can accelerate reaction and favour the formation of a higher coating volume $r = k\, C^{a}_{Cr^{+3}}\, C^{b}_{H_3PO_4}$, sufficiently covering the electrode. That is, during the initial period of coating, the rate of deposition will increase with increase in the above three variables. However, the excessive deposition rate tends to cause many more pores and makes the coating looser. The looser surface results in an increase in *Q*dl and a decease in *n*. A more depressed loop also appears after this period. Therefore excessive increase of the above three variables decreases the corrosion resistance. A thicker, porous coating also means a less protective layer as the porous coating is very permeable to water and aggressive ions. A differential O_2 or CO_2 or Cl^- concentration cell may also develop in the pores [26].

Phosphorous compounds are commonly used to inhibit corrosion in aqueous electrolyte [27]. Their use is relatively risk free due to their low toxicity. Previous results show that H_3PO_4 and Cr^{+3} deposited on the surface of Al 6063 alloy ameliorate corrosion in chloride media [23]. According to Pearson's Principle of Hard and Soft Acids and Bases [28], the Cr^{+3} ion is a typical hard Lewis acid. Phosphate is a typical hard Lewis base. The hard Lewis base (phosphate) is supposed to form very stable complex with the hard Lewis acid (Cr^{+3}). It can be concluded that the corrosion reaction of coatings formed with Cr^{+3} (hard Lewis acid) and phosphate (hard Lewis base) can be effectively inhibited. Another explanation for the improved corrosion inhibition of phosphoric acid with respect to Cr^{+3} coatings could be the fact that the solubility of the complex (Cr^{+3} and phosphate) in the corrosion medium is very low ($Ks = 2.4 \times 10^{-23}$). This lower solubility can suppress both the anodic and cathodic processes.

According to Fig. 3b and Table 3, it was found that depositing for 3 min is suitable as an initial phase because the reaction just starts. A drastic increase in the loop size was observed after this period. The impedance value has no significant change after 9 min. Initially, the coating covers only a small fraction of the surface and is highly porous, very thin and consists of a mixture of trivalent chromium and phosphate compounds, and other ions from the solution. This leads to a lower *n* and *R*ct, and therefore to a high capacitance. After this period, a thick layer, rich in trivalent chromium oxides and phosphate compounds is formed on

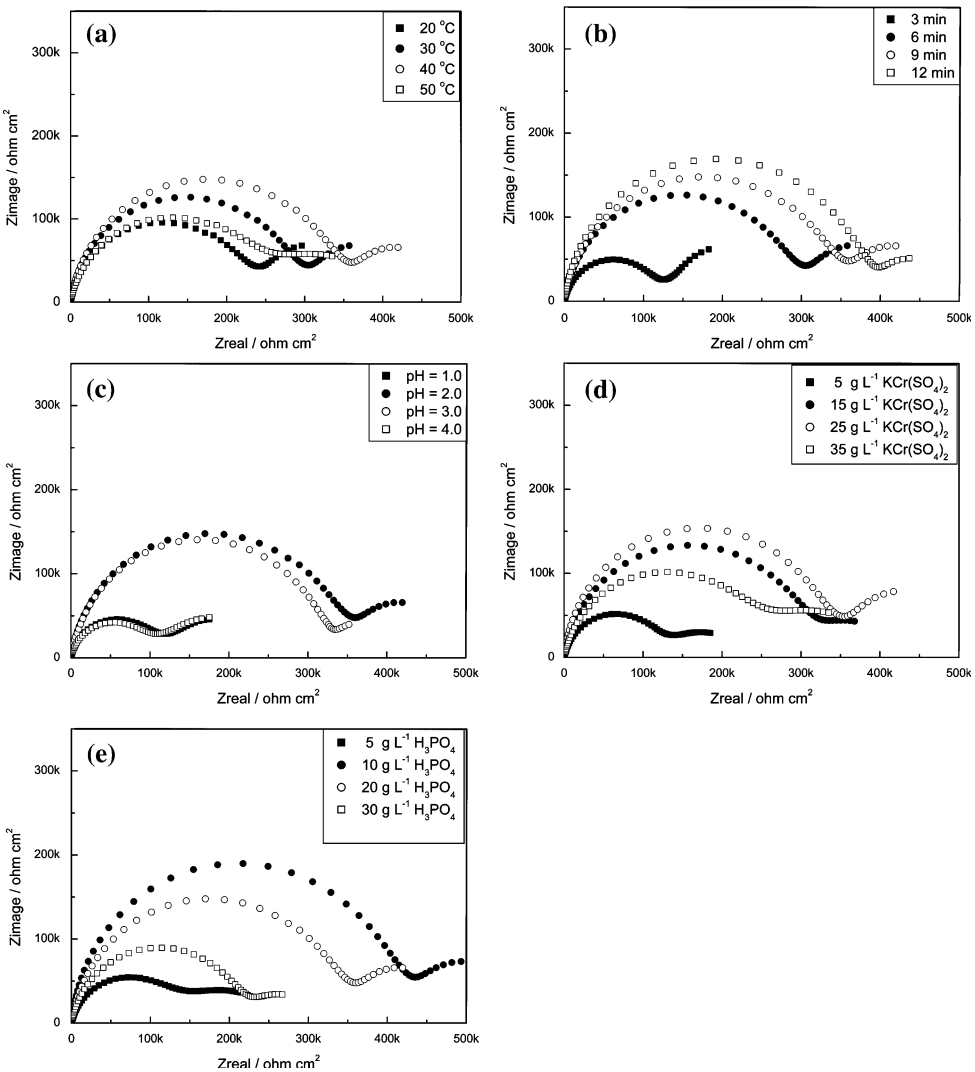

Fig. 3 Nyquist plots as functions of deposition (**a**) temperature, (**b**) time, (**c**) pH, and concentrations of (**d**) $KCr(SO_4)_2$ and (**e**) H_3PO_4 for aluminum 6063 alloy coated by Cr^{+3} conversion treatment. The other conditions were presented in Table 2

the pits, causing higher n and Rct values and a lower capacitance value. Depositing for 9 min seems to achieve an adequate corrosion resistance. Although the coating thickness increases with increasing time, the corrosion resistance is not completely proportional to thickness. Corrosion resistance depends on numerous factors, such as the composition, porosity, structure and thickness of coating, etc. The coating thickness presents a physical barrier against aggressive ions from the environment. When the other conditions remain constant, the corrosion resistance will be proportional to the coating thickness. Otherwise, the proportional relation will vary when the other factors, like the number of pores, vary. A longer reaction time tends to result in more pores. Moreover, industrial processes need to shorten the working time. Therefore, depositing for 9 min seems to provide the ideal reaction time.

It is interesting to note that the bath pH strongly affects the EIS of the coating as shown in the Nyquist plots (Fig. 3c) and Table 4. The charge transfer resistance (Rct) increases from 91.6 (pH = 4.0) to 321.6 kΩ cm^2 (pH = 3.0) and then abruptly decreases from 340.3 (pH = 2.0) to 99.2 kΩ cm^2 (pH = 1.0) with increasing the H^+ ion concentration. This suggests that the formation of the coating can be clearly divided into three stages. The first stage corresponds to the dominant formation process. The third stage is related to dissolution and pitting development. The middle stage (pH from 2.0 to 3.0) is considered to be a dynamic equilibrium region. The distinguished variation of EIS is due to competition result between the growth of precipitation, the increase in dissolution rate and the pore development. Furthermore, the lower pH gives more H_2 release ($2Al + 6H^+ \rightarrow 2Al^{3+} + 3H_2\uparrow$), and causes a rougher surface. This may be a contribution to the variation of Qdl from 0.39 (pH = 2.0) to 0.62 μF cm^{-2} (pH = 1.0) and n from 0.93 to 0.88.

According to the above analysis, the coating formed within the ranges, like temperature from 30 °C to 40 °C, depositing for 9 min, pH from 2.0 to 3.0, concentration of

Table 4 Fitting results with different concentrations

Concentration	Rs (Ω cm^2)	Qdl		Rct (kΩ cm^2)	Ws		
		C_{dl} (μF cm^{-2})	n		Rw (kΩ cm^2)	Cw (F cm^{-2})	n_w
pH							
4.0	43.6	0.62	0.88	91.6	161.5	40.0	0.39
3.0	43.8	0.42	0.91	321.6	90.6	41.6	0.50
2.0	46.6	0.39	0.91	340.3	139.9	41.2	0.50
1.0	42.9	0.62	0.88	99.2	151.3	40.0	0.40
[$KCr(SO_4)_2$] (g L^{-1})							
5	43.1	0.61	0.88	113.1	123.2	49.5	0.34
15	43.3	0.58	0.90	310.5	126.8	50.4	0.50
25	44.5	0.39	0.94	332.6	183.6	50.0	0.45
35	43.8	0.70	0.87	224.2	194.7	50.0	0.43
[H_3PO_4] (g L^{-1})							
5	44.4	0.81	0.86	112.4	163.2	44.9	0.30
10	44.6	0.38	0.94	413.5	165.8	45.0	0.50
20	46.6	0.39	0.91	340.3	139.9	41.2	0.50
30	44.3	0.61	0.88	213.9	112.5	49.6	0.41

$KCr(SO_4)_2$ from 15 to 25 g L^{-1}, and H_3PO_4 from 10 to 20 g L^{-1}, would give better corrosion resistance. Therefore the values of five variables have important influence on the roughness and corrosion resistance of the surface.

Generally, the high and intermediate frequency semicircle is believed to be caused by charge transfer before diffusion. The diffusion of Al ions from the electrode surface to bulk solution and the diffusion of dissolved oxygen from bulk solution to film surface occur in the low frequency region. Table 3 shows that the diffusion impedance value (Rw = 74.1 kΩ cm^2) of the uncoated alloy is much larger than its charge transfer resistance (Rct = 9.9 kΩ cm^2). This shows that the diffusion process can dominate the whole corrosion process for the uncoated Al alloy and also means that the uncoated sample easily suffers from attack by aggressive substances like carbon dioxide or chloride ions. The diffusion of Al ions and oxygen across pores and through the solution is very difficult in the low frequency region (below 0.5 Hz). From Tables 3 and 4, the Rct and Rw values of the coated sample are much larger than those of the uncoated. This suggests that electrochemical reaction is difficult on the coated electrode surface and the trivalent chromium coating presents better corrosion resistance. For aluminum alloys, corrosion mainly includes the following electrochemical activities: anodic dissolution and diffusion of Al ($Al \rightarrow Al^{3+} + 3e$), and diffusion and cathodic reduction of oxygen ($O_2 + 2H_2O + 4e \rightarrow 4OH^-$). The higher values of charge transfer resistance (Rct) and n, and the lower Qdl are a reflection of the thicker and denser coating which presents a barrier to O_2 or CO_2 or Cl^- permeation [26], thus protecting Al 6063 alloy from corrosion.

3.3 Surface morphology

A SEM image of the uncoated electrode is shown in Fig. 4a. The same electrode was coated under the second deposition condition shown in Table 2d. Figure 4b presents the SEM of the coated electrode. The surface of the uncoated electrode is full of pores and pits and is very rough. Figure 4b shows that the number of pores and pits is much lower. Although both the electrode surfaces are non-homogeneous, the surface of the coated electrode is more uniform and homogeneous than that of the uncoated. Therefore the SEM results further support the proposed model.

4 Conclusions

Surface modification by trivalent chromium coatings significantly improves the corrosion resistance of Al 6063 alloy. EIS reveals that the surface homogeneity and charge transfer resistance depend strongly on deposition temperature, time, concentrations of H^+ ions, trivalent-chrome compound and H_3PO_4. The optimal conditions were determined as follows: coating temperature 30–40 °C, deposition time 9 min, pH 2.0–3.0, the concentrations of $KCr(SO_4)_2$ and H_3PO_4 within 15–25 g L^{-1} and 10–20 g L^{-1}, respectively. Under such conditions, the surface roughness exhibits a minimum and the transfer resistance a maximum. Bath pH

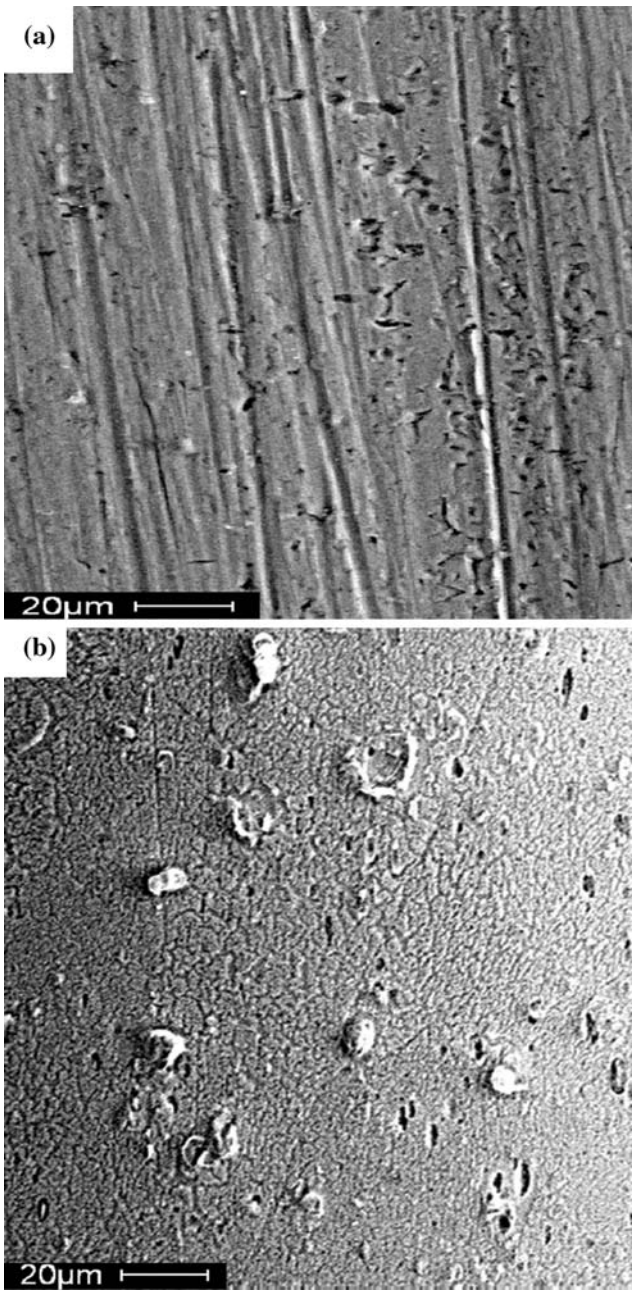

Fig. 4 SEM images of (**a**) the uncoated and (**b**) Cr^{+3} coated aluminum 6063 alloy electrodes

strongly affects the formation and quality of the coating. The equivalent circuit and the surface model were found to be consistent with the EIS spectra. Moreover, EIS and SEM were found to support the proposed model.

Acknowledgement This work was supported by the Natural Science Foundation of Hunan Province, China (No. 50175004).

References

1. Lancker VM (1967) Metallurgy of aluminium alloys. William Clowes and Sons, London
2. Mondolfo LF (1976) Aluminium alloys: structure and properties. Butterworths, London
3. Pardo A, Merino MC, Arrabal R, Feli′u S Jr, Viejo F, Carboneras M (2006) Electrochim Acta 51:4367
4. Deflorian F, Rossi S, Fedrizzi L, Bonora PL (2005) Prog Org Coat 52:271
5. Yu XW, Cao CN, Yao ZM, Zhao DR, Yin ZG (2000) Mater Sci Eng A284:56
6. Directive 2002/95/EC of the European Parliament and the Council on the Restriction of the Use of Certain Hazardous Substances in Electrical and Electronic Equipment (2003) Off J Eur Union, 27 Jan 2003
7. Hamdy AS (2006) Mater Lett 60:2633
8. Battocchi D, Simoes AM, Tallman DE, Bierwagen GP (2006) Corros Sci 48:2226
9. Yue TM, Yan LJ, Chan CP, Dong CF, Man HC, Pang GKH (2004) Surf Coat Technol 179:158
10. Mary Whitten C, Lin CT (2000) Prog Org Coat 38:151
11. Deck PD, Moon M, Sujdak RJ (1998) Prog Org Coat 34:39
12. Kok WH, Sun X, Shi L, Wong KC, Mitchell KAR (2001) J Mater Sci 36:3941
13. Hamdy AS, Beccaria A, Traverso P (2005) J Appl Electrochem 35:467
14. Bibber JW (2001) Met Finish 65(12):15
15. Li XQ, Cheng DQ, Yu QQ (2005) Chemical conversion coatings and its application, 1st edn. China Machine Press, Beijing (in Chinese)
16. Hamdy AS, Shoeib MA, Hady H, Abdel Salam OF (2008) J Appl Electrochem (in press). doi 10.1007/s10800-007-9451-9
17. Hassani Sh, Raeissi K, Golozar MA (2008) J Appl Electrochem (in press). doi 10.1007/s10800-008-9488-4
18. Sulka GD, Moshchalkov V, Borghs G, Celis JP (2007) J Appl Electrochem 37:789
19. Hasenay D, Seruga M (2007) J Appl Electrochem 37:1001
20. Hazzazi OA (2007) J Appl Electrochem 37:933
21. Bhatia P (2007) Corrosion resistant trivalent chromium phosphated chemical conversion coatings. US Patent 7,018,486, 20 Feb 2007
22. Diaddario LL, Marzano JM (2006) Trivalent chromate conversion coating. US Patent 7,029,541, 18 Feb 2006
23. Yu HC, Chen BZ, Shi XC, Sun XL, Li B (2008) Mater Lett 62:2828
24. Campestrini P, Van Westing EPM, De Wit JHW (2001) Electrochim Acta 46:2631
25. Levi MD, Wang C, Aurbach D (2004) J Electroanal Chem 561:1
26. Song FM, Jones DA, Kirk DW (2005) Corrosion 61(2):145
27. Rout TK, Bandyopadhyay N, Venugopalan T (2006) Surf Coat Technol 201:1022
28. Pearson RG (1968) J Chem Educ 45:581